Modulation of oligodendrocyte generation during a critical temporal window after NG2 cell division

Robert A. Hill[1,3], **Kiran D. Patel**[1], **Christopher M. Goncalves**[1], **Jaime Grutzendler**[3], and **Akiko Nishiyama**[1,2,*]

[1]Department of Physiology and Neurobiology, University of Connecticut, Storrs, CT

[2]Connecticut Stem Cell Institute, University of Connecticut, Farmington, CT

[3]Department of Neurology, Yale University School of Medicine, New Haven, CT

Abstract

Oligodendrocytes in the mammalian brain are continuously generated from NG2 cells throughout postnatal life. However it has remained unclear when the decision of NG2 cells to self-renew or differentiate into oligodendrocytes occurs after cell division. Using a combination of *in vivo* and *ex vivo* imaging and fate analysis of proliferated NG2 cells in fixed tissue, we demonstrate that in the postnatal developing mouse brain, the majority of divided NG2 cells differentiate into oligodendrocytes during a critical age-specific temporal window of 3–8 days. Importantly, within this time period, myelin and oligodendrocyte damage accelerated oligodendrocyte differentiation from divided cells, while whisker removal decreased the survival of divided cells in the deprived somatosensory cortex. These findings indicate that during the critical temporal window of plasticity, the fate of divided NG2 cells is sensitive to modulation by external signals.

Oligodendrocytes in the mammalian central nervous system (CNS) are generated from NG2 cells (also known as polydendrocytes or oligodendrocyte precursor cells (OPCs)). NG2 cells in rodent telencephalon appear in late gestation and continue to expand through the first two weeks of postnatal life. Even after peak oligodendrocyte production during the third postnatal week, NG2 cells persist as a uniformly distributed resident glial cell population in the adult CNS and retain their proliferative ability throughout life[1,2]. Recent genetic fate mapping studies revealed that NG2 cells continue to generate oligodendrocytes asynchronously throughout life, and those in white matter and younger mice differentiate faster than those in the gray matter and older mice[3–8].

A variety of signals from the neural microenvironment can modulate oligodendrocyte and myelin production[9,10]. For example, reduction in oligodendrocyte number induces rapid NG2 cell proliferation, ultimately leading to restoration of oligodendrocyte density[11]. Furthemore, blocking neuronal activity in culture or through social deprivation reduces myelination, while physical exercise increases oligodendrocyte differentiation[12–15]. Little is

*Corresponding author: Akiko Nishiyama, Department of Physiology and Neurobiology, University of Connecticut, Storrs, CT 06269, akiko.nishiyama@uconn.edu, Phone: 860-486-4561, Fax: 860-486-3303.

known, however, about the nature and the timing of the physiological signals that lead to the decision of divided NG2 cells to differentiate, self-renew, or die.

We previously showed that NG2 cells from early postnatal brain divide symmetrically to generate two daughter NG2 cells, which continue to express NG2 for several days before one or both differentiate into oligodendrocytes[6]. These observations suggested that the fate of divided NG2 cells may be determined by the microenvironment during this latency period. We have directly tested this hypothesis, using a combination of slice cultures, *in vivo* EDU pulse-chase labeling, and transcranial two-photon imaging of live mice carrying dual fluorescence reporters. We demonstrate that there is a critical temporal window between NG2 cell division and differentiation during which oligodendrocyte generation can be modulated by changes in their microenvironment. The latency between NG2 cell division and oligodendrocyte differentiation is shortened by myelin/oligodendrocyte damage. Moreover, sensory deprivation reduces the survival of divided NG2 cells that are in the process of differentiating into oligodendrocytes during this critical temporal window.

RESULTS

Stereotyped oligodendrocyte generation from divided NG2 cells

To determine the temporal dynamics of NG2 cell differentiation into oligodendrocytes after division *in vivo*, we first performed pulse-chase labeling with EDU in *NG2creER:YFP* mice that were double transgenic for tamoxifen-inducible *NG2creER* and the Cre reporter *gt(ROSA)26Sor^tm1(EYFP)Cos* (*YFP*). We injected 4-hydroxytamoxifen (4OHT) from postnatal day 6 to 8 (P6–P8) to induce YFP expression in NG2 cells, followed by a single EDU injection at P8. We sacrificed animals 2 hours (P8+0) or 1 (P8+1), 2 (P8+2), 3 (P8+3), and 4 (P8+4) days after EDU injection (Figure 1a). We determined the proportion of YFP+EDU+ cells that expressed the CC1 oligodendrocyte antigen at each time point in both the cortex and the corpus callosum (Figure 1b, e). The first emergence of YFP+EDU+CC1+ cells occurred at P8+2, suggesting that *in vivo* NG2 cells in both the cortex and corpus callosum take at least 48 hours after DNA replication to differentiate into CC1+ oligodendrocytes. The percentage of YFP+EDU+ cells that expressed CC1 increased and reached a plateau over the next two days. More than 40% of the divided cells differentiated into the CC1+ oligodendrocyte stage within 3 days after division (Figure 1e).

In addition to population analysis, we characterized the fate of single pairs of YFP+EDU+ cells in *NG2creER:YFP* mice. Three days of 4OHT injections at P8 gave an efficiency of Cre induction that was sufficiently low (25.7±1.5% in the cortex and 24.8±0.9% in the corpus callosum) that one could identify isolated pairs of YFP+EDU+ cells. Daughter cell pairs were defined as two cells that were YFP+EDU+ and were less than one cell body diameter away from each other (Figure 1c–d). At P8+3 and P8+4 we often observed YFP +EDU+ cell pairs with cell bodies very close to one another (for example see Figure 1e) and these cells often expressed CC1. Quantification revealed a greater proportion of cell pairs that consisted of two CC1+ cells (symmetric) in the corpus callosum than in the cortex (Figure 1d). Furthermore, the percentage of cell pairs resulting in asymmetric and/or symmetric CC1+ differentiation outcomes increased from P8+2 to P8+3 dpi but less prominently from P8+3 to P8+4 (Figure 1d).

We performed a similar experiment in P21 mice. We injected 4OHT from P18–P21 to induce (Cre induction efficiency, 12–70% in the cortex and 13–45% in the corpus callosum), followed by a single EDU injection at P21 (Figure 1a). We sacrificed animals at 1, 2, 4, 6, 8, and 10 days after EDU and determined the proportion of YFP+EDU+ cells that had differentiated into CC1+ oligodendrocytes in the corpus callosum and cortex (Figure 1f). There was a steep rise in the proportion of YFP+EDU+ that were also CC1+ between 2 and 4 days after EDU injection, which was followed by a more modest increase. In the cortex, the proportion of YFP+EDU+ cells that were CC1+ reached a plateau at 8 dpi at 48%, and there was no significant increase from 8 to 10 dpi (p>0.999). In the corpus callosum, the rate of increase in the proportion of YFP+EDU+ cells that were CC1+ also decreased beyond 6 dpi. However, unlike the cortex, the proportion of divided YFP+ cells that became oligodendrocytes continued to increase slightly (65% at 6 dpi, 73% at 8 dpi, and 80% at 10 dpi), although the increase between 8 and 10 dpi was not statistically significant. This suggested that at both P8 and P21, there was a temporal window after NG2 cell division during which the majority of the differentiation events occurred, although the duration of this window was longer in P21 mice.

In vivo imaging using dual reporter mice

We generated mice that were triple transgenic for NG2cre, expressing constitutively active Cre in NG2 cells, the cre reporter *Z/EG*, and *PLPDsRed*[16], which expresses DsRed under the control of the proteolipid protein promoter. In P21 *NG2cre:ZEG:PLPDsRed* triple heterozygous transgenic mice, GFP was detected in both NG2 cells (NG2+ PDGFRα+) and oligodendrocytes (CC1+), while DsRed was detected only in mature oligodendrocytes that expressed CC1 but not in NG2 cells expressing NG2 or PDGFRα (Figure 2a–f). DsRed+ cells first appeared in the corpus callosum at P6–P8 and their density steadily increased over the following weeks in both corpus callosum and deeper cortical layers (Figure 2g), whereas in cortical layer I they did not appear until P21–P23. While all PLPDsRed+ cells were CC1+, only a subpopulation of CC1+ cells were DsRed+ (Figure 2h, Supplementary Fig. 1), suggesting DsRed fluorescence is restricted to mostly to myelinating oligodendrocytes[17].

To investigate NG2 cell division and their differentiation dynamics *in vivo* we performed repeated transcranial two-photon fluorescence imaging in *NG2cre:ZEG:PLPDsRed* mice (Figure 3a, Supplementary Fig. 1). *NG2cre:ZEG* double transgenic mice express GFP in cells throughout the oligodendrocyte lineage in addition to vascular pericytes[18,19]. Pericytes were easily distinguished from oligodendroglial cells by their unique bipolar morphology and association with the vasculature visualized via intravenous (IV) injection of Texas Red dextran (Figure 3b arrows), while NG2 cells were identified by their distinct multi-processed morphology (Figure 3b arrowheads). Using *NG2cre:ZEG:PLPDsRed mice*, we captured image stacks beginning at P20–22 once a day for 10 days through layers I–III of the same region from the somatosensory cortex (Supplementary Movie 1). Excitation at 975nm wavelength effectively elicited both GFP and DsRed fluorescence, providing an *in vivo* dual reporter system to identify both NG2 cells and mature oligodendrocytes (Figure 3a, Supplementary Movie 1).

NG2 cells divide and translocate with variable trajectories

Analysis of the behavior of GFP+ cells in *NG2cre:ZEG* from P21–P32 mice revealed that while pericyte location remained highly stable, many NG2 cells translocated their cell bodies from day to day in the X, Y and Z dimensions. Many NG2 cells divided, and some underwent multiple cell divisions during the 10–12 day imaging session (Figure 3c, Supplementary Movie 2), consistent with previous reports of their proliferative properties [20,21]. We also observed many GFP+ cells disappearing (Figure 3d red X) or migrating out of the field of view (Figure 3d blue O, Supplementary Movie 3) over the imaging session, occurring either with or without a cell division. Quantification revealed similar numbers of dividing and disappearing cells per day in each of the four cortical depths. Out of 82 cells that were imaged in vivo over 10 days (P22–P31), 9.9% disappeared without division, 10.4% disappeared after division, 15.4% divided and did not disappear and 64.4% remained stable (Supplementary Fig. 1). Cell division followed by disappearance took place on average within 3.6 days after division (range 2–6 days) and cells that disappeared without division did so within 3.4 days (range 2–6 days) after the start of imaging. The total density of GFP+ cells over the imaging period remained remarkably stable over 10–12 days (Figure 3e).

We next determined if cell division and cell separation followed a stereotyped behavior by measuring the distance between individual divided cells 1 day after division had occurred. We found that separation was highly variable, ranging from 1.6 to 24.2μm, with an average of 8.5μm (Figure 3f). The distance between individual divided cells over multiple days also varied considerably, ranging from 5μm to 55μm within 5 days after division (Figure 3g).

Finally we sought to determine if NG2 cells divided in a specified division plane (Figure 3i). Out of 86 cell divisions that were imaged, 21%, 29%, 29% and 21% divided at an angle of 45°, 90°, 135° and 180°, respectively, relative to the pial surface (Figure 3h). These data suggested that the plane of division appeared to be random and was highly variable between individual cell division events.

Protracted differentiation after NG2 cell division in vivo

On the first day of *in vivo* imaging (P20–P22) DsRed+ cells were rarely detected in *NG2cre:ZEG:PLPDsRed* mice, consistent with fixed tissue analysis of DsRed developmental expression and with reported developmental myelination of cortical layers I–III imaged *in vivo* (Figure 4a–c)[17]. On subsequent days (up to P32), in addition to finding many GFP+ cells dividing and migrating over variable distances, we saw multiple GFP+ cells gradually becoming DsRed+ (Figure 4c, Supplementary Movie 4). Interestingly, over the 10–12 day imaging session we never observed a GFP+ cell that divided and then became DsRed+ (869 GFP+ cells imaged over 5–12 days in 4 mice). These data suggested that it takes more than 10 days for most of the divided NG2 cells to differentiate into oligodendrocytes in the neocortex of P21 mice. Quantification of total GFP+DsRed+ cells showed a gradual increase over time with the largest increase occurring in the upper most region (Figure 4d), consistent with myelination of layer I cortical axons.

To determine the region- and age- dependent temporal dynamics of oligodendrocyte maturation after NG2 cell division *in vivo*, we performed pulse-chase labeling with EDU in *PLPDsRed* mice after EDU injection at P8 (Supplementary Fig. 2a–c) or P21 (Supplementary Fig. 2d–f). EDU-injected mice were sacrificed 3, 4, 5, 6, 8, or 10 days post injection (dpi). In the P8 group, the first DsRed+EDU+ cells appeared at P8+4 in both the corpus callosum and cortex (Supplementary Fig. 2a–c), indicating that the onset of PLPDsRed fluorescence lags behind the onset of the expression of the CC1 antigen by approximately two days (compare with Figure 2h). In the corpus callosum, the proportion of DsRed+ cells labeled with EDU at P8 continued to increase and reached a plateau of 15% at 8 dpi. By contrast, in the neocortex the proportion of EDU+ DsRed+ cells remained below 1.5% (Supplementary Fig. 2c). In P21 mice, EDU+DsRed+ cells did not appear until 6 or 8 days after EDU injection in the corpus callosum and cortex, respectively (Supplementary Fig. 2d–f). In the cortex, 0, 0.7, and 3% of the EDU+ cells were DsRed+ at 6, 8, and 10 dpi, respectively. The majority of the DsRed+ cells were observed in deeper layers of the cortex. These data suggest that while terminal oligodendrocyte differentiation occurs during a critical temporal window after division, oligodendrocyte maturation and myelination proceeds gradually over a more extended time period.

Myelin damage accelerates differentiation after division

We next examined whether the time to oligodendrocyte differentiation after NG2 cell division could be altered by environmental conditions. NG2 cells are known to undergo enhanced proliferation and oligodendrocyte production in response to demyelination or developmental defects in myelin or oligodendrocyte production[22,23]. To model myelin and oligodendrocyte injury, we exposed forebrain slice cultures[24] from P8 *NG2cre:ZEG:PLPDsRed* mice to α–lysophosphatidylcholine (LPC), which causes and acute demyelinating injury in white matter followed by spontaneous remyelination (Supplementary Fig. 3)[23,25–28]. As in vivo, DsRed+ cells were found in both the cortex and corpus callosum of control slice cultures and were also GFP+ and CC1+ (Figure 5a). LPC exposure resulted in reduced and disorganized myelin and degenerated appearance of oligodendrocyte processes compared with robust parallel oligodendrocyte processes extended along axons seen in control slices (Figure 5b), while NG2 cell-like cells appeared relatively unaffected by LPC.

After vehicle or LPC exposure we performed time-lapse imaging on the slices to track the fate of dividing GFP+ cells as previously described[6]. Out of 16 divided pairs examined in the control slices, none of the daughter GFP+ cells became DsRed+ over the 78-hour imaging session, although we often observed GFP+ cells becoming DsRed+ without any division occurring (Figure 5c, Supplementary Figure 4, Supplementary Movies 5, 6). By contrast, after LPC treatment, 3 of 32 division events generated one daughter cell that became DsRed+ within the 78-hour imaging session, which was also CC1+ after fixation (Figure 5d, Supplementary Movie 7). Post hoc immunostaining revealed that in control slices, 15 of the 16 GFP+ cell divisions imaged generated two GFP+CC1– daughter cells, 1 generated one GFP+CC1+ daughter cell, and none of the division events generated two CC1+ daughter cells (Figure 5e). By contrast, among 32 GFP+ cell divisions imaged after LPC exposure, 19 generated two GFP+CC1– daughter cells, 12 generated one GFP+CC1+

daughter cell, and 1 generated two GFP+CC1+ daughter cells (Figure 5e). Statistical analysis revealed that LPC treatment resulted in a significant increase in the percentage of cell divisions with asymmetric OPC/oligodendrocyte fate ($p = 0.0168$, unpaired Student's *t*-test) (Figure 5e). These data suggest that the integrity or the density of myelin and oligodendrocytes regulated the timing of oligodendrocyte maturation after NG2 cell division.

To determine if division orientation might be more prominent in slice culture imaging experiments we analyzed the division plane in both control and LPC-treated slices (Supplementary Fig. 5). Out of 56 cell divisions imaged in the cortex and corpus callosum, the proportions of vertical vs. horizontal (relative to the tangent on the pial surface) divisions was not significantly different between control and LPC-treated slices (Supplementary Fig. 5b). Furthermore, the proportion of divided cells that became CC1+ did not differ between vertical vs. horizontal divisions (Supplementary Fig. 5c), although there was a slight trend for more horizontal divisions after LPC and a greater proportion of CC1+ progeny after horizontal division. Further experiments are necessary to ultimately determine if plane of division is a predictor of differentiation both in slice cultures and in vivo.

Sensory deprivation increases apoptosis of divided cells

We used the somatosensory barrel cortex to analyze if sensory deprivation caused by whisker clipping could influence the production of oligodendrocytes from divided NG2 cells. We injected *NG2creER:YFP* mice with 4OHT from P6 to P8 and clipped all the whiskers on the right side every day from P6 until the day of sacrifice 4 or 6 days later (Figure 6a-h, Supplementary Fig. 6), to target a developmental stage when the barrel structural plasticity critical period had ended and active cortical myelination was just beginning. The density of total CC1+ oligodendrocytes and YFP+CC1+ cells was significantly smaller in the deprived somatosensory cortex compared with the spared cortex at P6+4 and at P6+6 (Figure 6a–e). Furthermore the proportion of YFP+ cells that had become CC1+ oligodendrocytes was significantly lower in the deprived somatosensory cortex at P6+4 and P6+6 (Figure 6f). The effect of whisker clipping on oligodendrocyte density was specific to the somatosensory cortex, as we did not detect significant differences in the density of oligodendrocytes cells or the proportion of YFP+CC1+ cells at both time points between the deprived and spared motor cortex in the same sections adjacent to the somatosensory cortex (Supplementary Fig. 7b–d). These data suggested that whisker sensory input influences NG2 cell differentiation into oligodendrocytes during the second postnatal week.

We next investigated the effect of whisker clipping on oligodendrocyte differentiation after NG2 cell division. A single injection of EDU was given to *NG2creER:YFP* mice at P8 that had whiskers clipped unilaterally starting at P6 and 4OHT injected from P6–P8. Mice were perfused 2 and 4 days after EDU injections (P8+2 and P8+4) and the fate of YFP+EDU+ cells was determined in the spared and deprived somatosensory cortices. The density of CC1+EDU+ cells was significantly lower in deprived sides at P8+4 and the percentage of YFP+CC1+EDU+ cells out of all YFP+EDU+ cells was 5–fold lower in the deprived somatosensory cortex at both P8+2 and P8+4 compared with the spared somatosensory

cortex (Figure 6g–h) but there was no difference in the motor cortex (Supplementary Fig. 7e–f). When whisker clipping was performed in *PLPDsRed* mice, the density of DsRed+ cells was significantly lower in deprived sides 8 and 15 days after the start of clipping (Figure 6i–j). Furthermore, the density and percentage of divided cells (EDU+) that became DsRed+ was significantly lower in the deprived compared with the spared somatosensory cortex at 6 days after P8 EDU injection (Figure 6k–l). These data indicate that sensory deprivation significantly reduces oligodendrocyte production from divided NG2 cells during the window of time after division when differentiation into CC1+ oligodendrocytes plateaus under normal conditions. A two-hour pulse labeling of EDU revealed that NG2 cell proliferation was slightly higher in the deprived compared with spared somatosensory cortex at 4 (18% higher) and 6 days after initiation of whisker clipping (37% higher) (Figure 7a).

To determine whether the reduced oligodendrocyte production in the deprived cortex was caused by increased death of newly divided cells, we injected *NG2creER:YFP* mice with 4OHT from P6 to P8, clipped all the whiskers on the right side every day from P6 until P10, and performed a single injection of EDU at P8 (Figure 7b–e, Supplementary Fig. 6). Staining for active Caspase-3 in mice sacrificed at P8+2 revealed cells with typical apoptotic morphology (Figure 7c–f). The density of Caspase-3+ cells, Caspase-3+YFP+ cells, and Capase-3+EDU+ cells was significantly higher in the deprived cortex relative to the spared (Figure 7b). Caspase-3+CC1+ cells were present in both deprived and spared cortex, and there was no significant difference in their density (Figure 7b). While we did not detect Caspase-3+ in cells with typical NG2 cell morphology and strong PDGFRα immunoreactivity, there were Caspase-3+ round cells that had diffuse weak PDGFRα immunoreactivity (Figure 7d–e), some of which also had weak CC1 immunoreactivity. These findings suggested that sensory deprivation reduced the survival of divided NG2 cells that were in the process of differentiating into CC1+ oligodendrocytes.

DISCUSSION

Using a combination of *in vivo* and *ex vivo* imaging, cell fate mapping and EDU pulse-chase experiments, we demonstrated that during postnatal development, the fate of divided NG2 cells is determined within a critical temporal window between cell division and oligodendrocyte differentiation, the duration of which is region- and age-specific. At P8 the rate of oligodendrocyte differentiation from divided NG2 cells reached a plateau within 3–4 days. This temporal window between NG2 cell division and oligodendrocyte differentiation also existed in P21 mice but was protracted to 6–8 days. Interestingly, this plateau effect seemed to be more pronounced for cells in the cortex, whereas there was a trend for divided NG2 cells in the corpus callosum to continue to generate oligodendrocytes beyond the period of rapid oligodendrocyte production. Newly generated CC1+ oligodendrocytes subsequently matured and acquired PLPDsRed fluorescence over the following days, and the length of time from division to oligodendrocyte maturation was longer in P21 animals and in the cortical gray matter compared to the corpus callosum. Most importantly, we demonstrated that the temporal window between NG2 cell division and oligodendrocyte production represents a period when the divided cells are sensitive to fate modulation by external signals. Specifically, damage to myelin or oligodendrocytes accelerated the

differentiation after division, while a loss in sensory input compromised the survival of divided cells that were transitioning into oligodendrocytes.

Our observations from *in vivo* and slice culture imaging and EDU pulse-chase labeling followed by analysis of fixed brains collectively suggest that NG2 cells initially undergo symmetrical division into two daughter NG2 cells, which remain as NG2 cells for a few days before one differentiates into an oligodendrocyte. This is consistent with an earlier BrdU pulse-chase study in adult[21]. By contrast, a recent study reported that the NG2 protein was asymmetrically distributed during cell division, suggesting that the differentiation process begins immediately after division[29]. Although reasons for these contradictory findings are not clear, they could arise from differences in the age of the animals or the clonal preculture conditions[29].

NG2cre:ZEG:PLPDsRed triple transgenic mice allowed us to directly visualize the entire oligodendrocyte lineage and follow differentiation for the first time in a living mouse. During the 10 days of imaging, we did not detect DsRed fluorescence in the progeny of divided cells, even though DsRed fluorescence increased in intensity over time in oligodendrocyte lineage cells that had not divided during the imaging period. This was also evident with the EDU pulse-chase labeling of P21 *PLPDsRed* mice, which showed that fewer than 4% of the EDU+ cells became DsRed+ even 10 days after EDU labeling. Unlike embryonic neural progenitor cells, the progeny of divided NG2 cells remain as two daughter NG2 cells for several days to weeks after division depending on the age of the animal[6,21,30,31]. This was also noted by *in vivo* imaging of live adult *NG2-mEGFP* mice, although oligodendrocytes were not directly labeled[32]. The constitutive *NG2cre* rather than inducible *NG2creER* mice provided a good model despite the presence of GFP throughout the lineage since we were focused on the fate of dividing NG2 cells, and they enabled us to sample a large number of cell division events. The findings from this mouse line were consistent with those from the EDU pulse-chase experiments performed in the *NG2creER line*. Future studies could be conducted with additional new mouse lines to further define and investigate the temporal window.

A recent live imaging study in zebrafish reported that the number of myelin sheaths that an oligodendrocyte makes is determined during a relatively short time frame after initial contact with unmyelinated axons[33]. Our temporal analyses revealed another critical temporal window that occurs earlier between NG2 cell division and terminal oligodendrocyte differentiation, during which the fate of divided cells is influenced by their microenvironment. Our data suggests that cell intrinsic changes, such as chromatin remodelling[34] or oscillation of transcription factors such as Olig2[35], may be occurring in the divided NG2 cells during this "sensitivity window", which could alter the ability of the cell to respond to extracellular differentiation cues. Further investigation of the intracellular changes that occur in NG2 cells after division may shed light on whether all divided NG2 cells maintain the competence of differentiating into oligodendrocytes or whether some NG2 cells are programmed to permanently remain as NG2 cells.

The discovery of the narrow window of time between cell division and oligodendrocyte differentiation led us to investigate whether changes in external environment could modulate

the fate of the divided cells. Using live imaging of slice cultures, we observed that a subset of divided NG2 cells in LPC-treated slices matured into DsRed+ oligodendrocytes faster than under control conditions. Thus the time to oligodendrocyte differentiation after NG2 cell division is plastic and can be altered when oligodendrocyte production is necessary, suggesting a sensing mechanism that enables NG2 cells to detect changes in myelin or oligodendrocyte density or the presence of axons that would normally be myelinated. This hypothesis is supported by acute time-lapse imaging in zebrafish, which has shown that oligodendrocyte progenitors proliferate and replace laser-ablated oligodendrocytes[36], as well as the increased rate of oligodendrocyte generation from proliferated NG2 cells in the hypomyelinating mutant *shiverer* [22].

We have found for the first time that deprivation of whisker sensory input reduces oligodendrocyte production after NG2 cell division specifically in the deprived somatosensory cortex and not in the neighboring motor cortex. We previously reported that when whiskers were removed shortly after birth before the end of the critical period for structural plasticity, there were no changes in the distribution of NG2 cells or the NG2 molecule in the somatosensory cortex[37], while another study reported an increase in NG2 cell proliferation after whisker removal during the same developmental window[38]. In the current study, we found a modest increase in NG2 cell proliferation after whisker clipping. However, immunolabeling for active Caspase-3 revealed a 4.5-fold higher density of Caspase-3+ YFP+ cells in the deprived cortex than that in the spared cortex suggesting that the increase in NG2 cell proliferation does not result in a sustained increase in oligodendrocyte lineage cell density. The density of YFP+ Caspase-3+ cells in the deprived cortex (240 per mm^3) accounts for only one-third of the difference in the density of YFP+ CC1+ cells between the deprived and spared cortex (320 per mm^3 in deprived and 1164 per mm^3 in spared). It is likely that Caspase-3 immunolabeling detected only a subpopulation of the cells that were dying due to the short duration of the cell death process and rapid clearing of the dead cells. The density of Caspase-3+ CC1+ cells did not differ between deprived and spared cortex, which suggests that a certain fraction of differentiated oligodendrocytes die under normal conditions (0.55% Caspase-3+CC1+ / CC1+ at P10), although the fraction of Caspase-3+ cells was considerably lower than that the 50% rate reported for apoptotic cells in the optic nerve[39]. By contrast, the fraction of newly generated oligodendrocytes that were Caspase-3+ (YFP+CC1+) was significantly higher at 3.53%. The effect of sensory deprivation was most pronounced in the newly divided cells. Caspase-3+ cells that were also EDU+ were found only in the deprived cortex, where Caspase-3 was detected in cells with a round morphology and diffuse PDGFRα immunoreactivity or YFP+ cells that were neither PDGFRα+ nor CC1+. These observations suggest that sensory deprivation specifically affects divided cells that are in the process of terminally differentiating into oligodendrocytes and have downregulated PDGFRα but not yet acquired CC1, consistent with reports for the normal CNS showing cell death of newly differentiated oligodendrocytes[39,40].

Physiological neuronal activity could influence the survival of divided NG2 cells that are in the process of differentiating into oligodendrocytes by enhanced secretion of growth and trophic factors[40]. Brain-derived neurotrophic factor (BDNF) is known to be secreted by

neurons in an activity-dependent manner[41] and has been shown to promote proliferation and differentiation of oligodendrocyte lineage cells[42], although axotomy resulted in inconsistent effects on the survival of oligodendrocyte lineage cells in the optic nerves[43,44]. Live imaging of slice cultures revealed a slightly lower proportion of divided NG2 cells that differentiated into CC1+ oligodendrocytes compared with the corresponding values obtained *in vivo* over similar time frames. This could in part be explained by the absence of a fully functional neural circuit in the slices cultures compromising neuronal activity-dependent signals that direct divided NG2 cells to terminally differentiate rather than self-renew. As a whole, our observations demonstrate for the first time that decrease of peripheral sensory input by non-invasive methods leads to increased death of divided NG2 cells that are undergoing terminal oligodendrocyte differentiation.

Neuronal activity has been shown to positively influence NG2 cell differentiation and local myelin production *in vitro*[12,13,45,46]. *In vivo* rodent studies have also demonstrated that pharmacological manipulations or artificial electrical or optogenetic stimulation can influence NG2 cell differentiation[12,47]. In more physiological experiments, social isolation reduced myelination in the prefrontal cortex[14,15], while physical exercise increased the production of oligodendrocytes with a concomitant decrease in NG2 cell proliferation[48]. While these studies have revealed activity-dependent effects on oligodendrocyte differentiation, our EDU pulse-chase study revealed that sensory input influences the production of oligodendrocytes specifically in the deprived somatosensory cortex by locally regulating cell death during a discrete temporal window after NG2 cell division. The combination of EDU pulse-chase labeling with Caspase-3 labeling has provided the sensitivity to uncover a previously unrecognized mechanism of activity-dependent regulation of local oligodendrocyte production.

In summary, we have identified a critical temporal window after NG2 cell division during which the cells are susceptible to environmental factors that affect their oligodendrocyte differentiation or survival. This is the first demonstration that the critical temporal window can be altered by changes in myelin/oligodendrocyte health and that the survival of recently divided cells that are in the process of differentiating into oligodendrocytes can be modulated during the critical time window by alterations in physiological neuronal activity.

ONLINE METHODS

Animals and induction of Cre mediated recombination

For differentiation experiments, we used both male and female mice that were triple transgenic for *NG2creBAC*[18,19] (Jackson Labs #008533), the Cre reporter *Z/EG*[49] (Jackson Labs #003920), and *PLPDsRed*[16] (*NG2cre:ZEG:PLPDsRed*). *PLPDsRed* mice used in this study[16] were generated using the same *Plp* promoter construct that had previously been used to generate *PLP-EGFP* mice, in which 95% of the GFP+ cells were CC1+ oligodendrocytes[50]. Thus, unlike other *PLP-EGFP* mice generated with the 3'-untranslated region of the *Plp* gene and express EGFP in NG2 cells as well as in oligodendrocytes[51], DsRed fluorescence in the *PLPDsRed* mice was seen mostly in myelinating oligodendrocytes[17] and was not found in NG2 cells or immature oligodendrocytes (see Figure 2). For EDU pulse-chase and whisker removal experiments male and female

inducible double heterozygous for *NG2creER*[6] (Jackson Labs #008538) and *gt(ROSA)26Sor*[tm1(EYFP)Cos] (Jackson Labs #006148) mice (*NG2creER:YFP*) were used. Cre was induced in P6–8 mice by daily intraperitoneal injections of 0.2mg 4-hydroxytamoxifen (4OHT, Sigma) as described previously[6]. To label cells in the S phase of the cell cycle, one intraperitoneal injection of 5 μg/g of 5-ethynyl-2'-deoxyuridine (EDU, Life Technologies Cat#C10338) was administered. Animals were housed in a 12/12 hour light/dark cycle and housed in litters of 4–8 before weaning age (P21) and housed at a density of 2–5 per cage after weaning. All animal procedures were approved by the Institutional Animal Care and Use Committees (IACUC) at the University of Connecticut and Yale University.

In vivo two-photon imaging

For chronic transcranial time-lapse imaging, the thin skull procedure was used[52]. P20–22 *NG2cre:ZEG* and *NG2cre:ZEG:PLPDsRed* mice were anesthetized by intraperitoneal injection of ketamine and xylazine, and the scalp was shaved and sterilized. A region of the skull approximately 1 mm in diameter was thinned with a high speed drill and a microsurgical blade to a thickness of 20–30μm. Images were acquired using a two-photon microscope (Prairie Technologies) with a mode locked MaiTai tunable near infrared laser (Spectra Physics) and a 20x water immersion objective with a numerical aperture of 1.0 (Leica). In some cases 70,000 MW Texas Red dextran (Life Technologies) was intravenously injected to visualize the cortical vasculature. The following wavelengths were used for two-photon fluorescence excitation: 900nm for GFP alone, 975nm for GFP and DsRed, and 1040nm for DsRed alone. Z stacks of the same cortical region over a depth of 200–320μm with a 4μm step size were captured through the thinned skull on consecutive days at intervals depicted in the text. Images were analyzed using ImageJ.

Slice culture preparation and ex vivo time-lapse imaging

Forebrain slice cultures were prepared as described previously[6,24]. Briefly, 300μm coronal forebrain sections from P8 *NG2cre:ZEG:PLPDsRed* triple transgenic mice were placed on 0.45μm Millicell culture inserts (Millipore) and maintained in a humidified 37°C, 5% CO_2 incubator. Slice media consisted of: 50% Minimal Essential Medium with Earle's Salts containing 25 mM HEPES pH 7.22 and no L-glutamine; 25% Hank's Buffered Salt Solution without calcium or magnesium; 25% horse serum; 0.4mM ascorbic acid; 1mM L-glutamine; and 1mg/L insulin. Culture medium was changed 24 hours after dissection and every other day thereafter. For time-lapse imaging, several fields in each slice were manually imaged at 4-hour intervals with a 10x objective using a Zeiss Axiovert 200 M inverted microscope equipped with an ORCA ER camera. The slices were maintained in the incubator between imaging. At the end of the incubation, slices were fixed in 4% paraformaldehyde containing 0.1M L-Lysine and 0.01M sodium metaperiodate for 30 minutes (PFA-PLP fix; McLean and Nakane, 1974), and processed for immunohistochemistry using anti-GFP and CC1 antibodies.

LPC exposure in slice cultures

Cortical slice cultures from P8 *NG2cre:ZEG:PLPDsRed* triple transgenic mice were exposed to 0.5mg/mL α-lysophosphatidylcholine (LPC, lysolecithin) after 3 DIV to cause an

acute injury to myelin/oligodendrocyte membranes. After the 17 hours in LPC, the slices were returned to normal slice culture medium. Time-lapse imaging was started on 5 DIV, and images were manually taken every 4 hours for a total of 78 hours. Slices were then fixed with PFA-PLP and processed for immunohistochemistry using anti-GFP and CC1 antibodies.

Animal perfusions and immunohistochemistry

Animals were anesthetized with isoflurane and transcardially perfused with PFA-PLP fix. Brains were post-fixed for one hour in the same solution followed by 4 washes in 0.2M sodium phosphate buffer. Fifty-micrometer vibratome sections were cut and processed for immunohistochemistry. If antigen retrieval was necessary, sections were microwaved for 5 minutes in pH 6.0 sodium citrate buffer, cooled to room temperature, and then washed in phosphate-buffered saline (PBS). After blocking and permeabilizing for 1 hour in 5% normal goat serum (NGS) and 0.1% Triton X-100 in PBS, slices were incubated at 4°C overnight with primary antibodies diluted in PBS containing 5% NGS. Primary antibodies used were rabbit anti-NG2 antibody (Chemicon Cat#AB5320, 1:500), chicken anti-GFP antibody (Aves Labs Cat#GFP-1020, 1:500), mouse antibody to adenomatous polyposis coli antigen (APC; clone CC1, Calbiochem Cat#OP80 1:200), goat anti-PDGFRα antibody (R&D Systems Cat#AF1062, 1:500), rabbit anti-active Caspase-3 antibody (Abcam Cat# AB13847, 1:200) and AA3 rat monoclonal antibody that recognizes both DM20 and PLP splice variants of the *Plp* gene (Yamamura et al., 1991; obtained from Dr. Kaz Ikenaka, Okazaki, Japan). After PBS wash, slices were incubated in secondary antibodies at room temperature for 1 hour in PBS containing 5% NGS. Secondary antibodies used were Alexa 488-conjugated antibodies (Molecular Probes, 1:500), Cy3-conjugated antibodies (Jackson ImmunoResearch, 1:500), and Dylight 649-conjugated antibodies (Jackson ImmunoResearch 1:200). Detection of EDU was performed following PBS wash according to the manufacturer's protocol. Slices were then mounted on glass slides in Vectashield mounting medium (Vector Laboratories) containing 4',6-diamidino-2-phenylindole (DAPI). Fixed tissue imaging was performed using either a Zeiss Axiovert 200 M microscope with an ORCA ER camera (Hamamatsu) and Apotome grid confocal system or Leica SP2 and SP5 (Yale) confocal microscopes.

Whisker trimming and analysis of NG2 cell differentiation

The right whiskers of *NG2creER:YFP* or *PLPDsRed* animals were first trimmed at postnatal day 6 (P6) and 4OHT was injected into *NG2creER:YFP* mice from P6–P8. In some mice a single injection of EDU was also administered at P8. Whiskers were trimmed every day until the date of perfusion between P10 and P21. Sections from *NG2creER:YFP* mice were labeled for EDU, GFP, and CC1 or NG2, and the phenotype of YFP+ cells or YFP+EDU+ cells was analyzed. Sections from *PLPDsRed* mice were labeled for EDU only, and the EDU+ cells were scored for DsRed fluorescence.

Quantification and Statistics

For EDU pulse chase experiments with *NG2creER:YFP* and *PLPDsRed* transgenic mice, fluorescence reporter+, EDU+ and NG2 or CC1+ cells were quantified in both the cortex

and corpus callosum by randomly selecting regions with a defined area grid. Littermates were randomly assigned to each age group. At least four separate fields were quantified for each brain region in each section, and at least three sections were quantified for each mouse. For slice culture imaging, slices were prepared from 3 separate mice and 5 slices were analyzed for control conditions and 8–9 slices were analyzed for LPC. For *in vivo* imaging experiments, image stacks were compiled into time-lapse videos and analysis of cell density, division, division orientation, migration, disappearance, and differentiation was manually noted in specified 80-μm z-projections indicated in the text. For whisker manipulation experiments, cell quantification was blindly performed in layer IV of the contralateral and ipsilateral somatosensory and motor cortices. For all experiments data was compiled and analyzed from at least 3 animals for each age, genotype, time point, and condition. For each brain area to be quantified, unbiased quantification was performed by randomly sampling 4 fields of view based on DAPI staining and then the other florescence channels for quantification. Two way ANOVA analyses with Bonferroni post hoc analyses were performed on data acquired from age and region dependent EDU pulse chase experiments (Figures 1 and Supplementary Fig. 2). Unpaired or paired two-tailed Student's *t*-test analyses were performed for comparison of control and LPC treated slice cultures (Figure 5, Supplementary Fig. 5) and spared and deprived somatosensory and motor cortices (Figures 6–7 and Supplementary Fig.7) assuming equal variance between groups. Using Minitab, the sample sizes used in the experiments were calculated to give a power of analysis of 80% or greater based on the differences and standard deviations, assuming an alpha = 0.05. Data distribution was assumed to be normal but this was not formally tested. Representative images are examples of images used for quantification. The values reported for quantification and statistics between groups indicate how many times the experiment was successfully repeated.

Supplementary Material

Refer to Web version on PubMed Central for supplementary material.

ACKNOWLEDGEMENTS

References

1. Nishiyama A, Komitova M, Suzuki R, Zhu X. Polydendrocytes (NG2 cells): multifunctional cells with lineage plasticity. Nat. Rev. Neurosci. 2009; 10:9–22. [PubMed: 19096367]

2. Hill RA, Nishiyama A. NG2 cells (polydendrocytes): Listeners to the neural network with diverse properties. Glia. 2014; 62:1195–1210. [PubMed: 24753030]

3. Dimou L, Simon C, Kirchhoff F, Takebayashi H, Gotz M. Progeny of Olig2-expressing progenitors in the gray and white matter of the adult mouse cerebral cortex. J. Neurosci. 2008; 28:10434–10442. [PubMed: 18842903]

4. Kang SH, Fukaya M, Yang JK, Rothstein JD, Bergles DE. NG2+ CNS glial progenitors remain committed to the oligodendrocyte lineage in postnatal life and following neurodegeneration. Neuron. 2010; 68:668–681. [PubMed: 21092857]

5. Rivers LE, et al. PDGFRA/NG2 glia generate myelinating oligodendrocytes and piriform projection neurons in adult mice. Nat. Neurosci. 2008; 11:1392–1401. [PubMed: 18849983]

6. Zhu X, et al. Age-dependent fate and lineage restriction of single NG2 cells. Development. 2011; 138:745–753. [PubMed: 21266410]

7. Viganò F, Möbius W, Götz M, Dimou L. Transplantation reveals regional differences in oligodendrocyte differentiation in the adult brain. Nat. Neurosci. 2013; 16:1370–1372. [PubMed: 23995069]

8. Young KM, et al. Oligodendrocyte Dynamics in the Healthy Adult CNS: Evidence for Myelin Remodeling. Neuron. 2013; 77:873–885. [PubMed: 23473318]

9. Chong SYC, Chan JR. Tapping into the glial reservoir: cells committed to remaining uncommitted. J. Cell Biol. 2010; 188:305–12. [PubMed: 20142420]

10. Zuchero JB, Barres BA. Intrinsic and extrinsic control of oligodendrocyte development. Curr. Opin. Neurobiol. 2013; 23:914–920. [PubMed: 23831087]

11. Nishiyama A. Polydendrocytes: NG2 cells with many roles in development and repair of the CNS. Neuroscientist. 2007; 13:62–76. [PubMed: 17229976]

12. Demerens C, et al. Induction of myelination in the central nervous system by electrical activity. Proc. Natl. Acad. Sci. U. S. A. 1996; 93:9887–9892. [PubMed: 8790426]

13. Malone M, et al. Neuronal activity promotes myelination via a cAMP pathway. Glia. 2013; 61:843–54. [PubMed: 23554117]

14. Liu J, et al. Impaired adult myelination in the prefrontal cortex of socially isolated mice. Nat. Neurosci. 2012; 15:1621–3. [PubMed: 23143512]

15. Makinodan M, Rosen KM, Ito S, Corfas G. A critical period for social experience-dependent oligodendrocyte maturation and myelination. Science. 2012; 337:1357–60. [PubMed: 22984073]

16. Hirrlinger PG, et al. Expression of reef coral fluorescent proteins in the central nervous system of transgenic mice. Mol. Cell. Neurosci. 2005; 30:291–303. [PubMed: 16169246]

17. Schain AJ, Hill RA, Grutzendler J. Label-free in vivo imaging of myelinated axons in health and disease with spectral confocal reflectance microscopy. Nat. Med. 2014; 20:443–9. [PubMed: 24681598]

18. Zhu X, Bergles DE, Nishiyama A. NG2 cells generate both oligodendrocytes and gray matter astrocytes. Development. 2008; 135:145–157. [PubMed: 18045844]

19. Zhu X, Hill RA, Nishiyama A. NG2 cells generate oligodendrocytes and gray matter astrocytes in the spinal cord. Neuron Glia Biol. 2008; 4:19–26. [PubMed: 19006598]

20. Psachoulia K, Jamen F, Young KM, Richardson WD. Cell cycle dynamics of NG2 cells in the postnatal and ageing brain. Neuron Glia Biol. 2009; 5:57–67. [PubMed: 20346197]

21. Dawson MR, Polito A, Levine JM, Reynolds R. NG2-expressing glial progenitor cells: an abundant and widespread population of cycling cells in the adult rat CNS. Mol. Cell. Neurosci. 2003; 24:476–488. [PubMed: 14572468]

22. Bu J, Banki A, Wu Q, Nishiyama A. Increased NG2(+) glial cell proliferation and oligodendrocyte generation in the hypomyelinating mutant shiverer. Glia. 2004; 48:51–63. [PubMed: 15326615]

23. Watanabe M, Toyama Y, Nishiyama A. Differentiation of proliferated NG2-positive glial progenitor cells in a remyelinating lesion. J. Neurosci. Res. 2002; 69:826–36. [PubMed: 12205676]

24. Hill RA, Patel KD, Medved J, Reiss AM, Nishiyama A. NG2 Cells in White Matter But Not Gray Matter Proliferate in Response to PDGF. J. Neurosci. 2013; 33:14558–14566. [PubMed: 24005306]

25. Birgbauer E, Rao TS, Webb M. Lysolecithin induces demyelination in vitro in a cerebellar slice culture system. J. Neurosci. Res. 2004; 78:157–166. [PubMed: 15378614]

26. Fancy SP, et al. Axin2 as regulatory and therapeutic target in newborn brain injury and remyelination. Nat. Neurosci. 2011; 14:1009–1016. [PubMed: 21706018]

27. Hall SM. The effect of injections of lysophosphatidyl choline into white matter of the adult mouse spinal cord. J. Cell Sci. 1972; 10:535–546. [PubMed: 5018033]

28. Gensert JM, Goldman JE. Endogenous progenitors remyelinate demyelinated axons in the adult CNS. Neuron. 1997; 19:197–203. [PubMed: 9247275]

29. Sugiarto S, et al. Asymmetry-defective oligodendrocyte progenitors are glioma precursors. Cancer Cell. 2011; 20:328–340. [PubMed: 21907924]

30. Kukley M, et al. Glial cells are born with synapses. FASEB J. 2008; 22:2957–2969. [PubMed: 18467596]

31. Ge WP, Zhou W, Luo Q, Jan LY, Jan YN. Dividing glial cells maintain differentiated properties including complex morphology and functional synapses. Proc. Natl. Acad. Sci. U. S. A. 2009; 106:328–333. [PubMed: 19104058]

32. Hughes EG, Kang SH, Fukaya M, Bergles DE. Oligodendrocyte progenitors balance growth with self-repulsion to achieve homeostasis in the adult brain. Nat. Neurosci. 2013; 16:668–76. [PubMed: 23624515]

33. Czopka T, Ffrench-Constant C, Lyons DA. Individual Oligodendrocytes Have Only a Few Hours in which to Generate New Myelin Sheaths In Vivo. Dev. Cell. 2013; 25:599–609. [PubMed: 23806617]

34. Liu J, Casaccia P. Epigenetic regulation of oligodendrocyte identity. Trends Neurosci. 2010; 33:193–201. [PubMed: 20227775]

35. Imayoshi I, et al. Oscillatory control of factors determining multipotency and fate in mouse neural progenitors. Science. 2013; 342:1203–8. [PubMed: 24179156]

36. Kirby BB, et al. In vivo time-lapse imaging shows dynamic oligodendrocyte progenitor behavior during zebrafish development. Nat. Neurosci. 2006; 9:1506–11. [PubMed: 17099706]

37. Hill RA, Natsume R, Sakimura K, Nishiyama A. NG2 cells are uniformly distributed and NG2 is not required for barrel formation in the somatosensory cortex. Mol. Cell. Neurosci. 2011; 46:689–698. [PubMed: 21292011]

38. Mangin J-M, Li P, Scafidi J, Gallo V. Experience-dependent regulation of NG2 progenitors in the developing barrel cortex. Nat. Neurosci. 2012; 15:1192–4. [PubMed: 22885848]

39. Barres BA, et al. Cell death and control of cell survival in the oligodendrocyte lineage. Cell. 1992; 70:31–46. [PubMed: 1623522]

40. Trapp BD. Differentiation and Death of Premyelinating Oligodendrocytes in Developing Rodent Brain. J. Cell Biol. 1997; 137:459–468. [PubMed: 9128255]

41. Marty S, Berzaghi MdaP & Berninger B. Neurotrophins and activity-dependent plasticity of cortical interneurons. Trends Neurosci. 1997; 20:198–202. [PubMed: 9141194]

42. VonDran MW, Singh H, Honeywell JZ, Dreyfus CF. Levels of BDNF impact oligodendrocyte lineage cells following a cuprizone lesion. J. Neurosci. 2011; 31:14182–90. [PubMed: 21976503]

43. Barres BA, Jacobson MD, Schmid R, Sendtner M, Raff MC. Does oligodendrocyte survival depend on axons? Curr. Biol. 1993; 3:489–97. [PubMed: 15335686]

44. Ueda H, Levine JM, Miller RH, Trapp BD. Rat optic nerve oligodendrocytes develop in the absence of viable retinal ganglion cell axons. J. Cell Biol. 1999; 146:1365–1374. [PubMed: 10491397]

45. Stevens B, Tanner S, Fields RD. Control of myelination by specific patterns of neural impulses. J. Neurosci. 1998; 18:9303–11. [PubMed: 9801369]

46. Wake H, Lee PR, Fields RD. Control of local protein synthesis and initial events in myelination by action potentials. Science. 2011; 333:1647–1651. [PubMed: 21817014]

47. Gibson EM, et al. Neuronal activity promotes oligodendrogenesis and adaptive myelination in the mammalian brain. Science. 2014; 344:1252304. [PubMed: 24727982]

48. Simon C, Gotz M, Dimou L. Progenitors in the adult cerebral cortex: cell cycle properties and regulation by physiological stimuli and injury. Glia. 2011; 59:869–881. [PubMed: 21446038]

49. Novak A, Guo C, Yang W, Nagy A, Lobe CG. Z/EG, a double reporter mouse line that expresses enhanced green fluorescent protein upon Cre-mediated excision. Genes. (New York, N.Y. 2000). 2000; 28:147–155.

50. Fuss B, et al. Purification and analysis of in vivo-differentiated oligodendrocytes expressing the green fluorescent protein. Dev. Biol. 2000; 218:259–74. [PubMed: 10656768]

51. Mallon BS, Shick HE, Kidd GJ, Macklin WB. Proteolipid promoter activity distinguishes two populations of NG2-positive cells throughout neonatal cortical development. J. Neurosci. 2002; 22:876–85. [PubMed: 11826117]

52. Grutzendler J, Kasthuri N, Gan W-B. Long-term dendritic spine stability in the adult cortex. Nature. 2002; 420:812–6. [PubMed: 12490949]

53. McLean IW, Nakane PK. Periodate-lysine-paraformaldehyde fixative. A new fixation for immunoelectron microscopy. J. Histochem. Cytochem. 1974; 22:1077–1083. [PubMed: 4374474]

54. Yamamura T, Konola JT, Wekerle H, Lees MB. Monoclonal antibodies against myelin proteolipid protein: identification and characterization of two major determinants. J. Neurochem. 1991; 57:1671–80. [PubMed: 1717653]
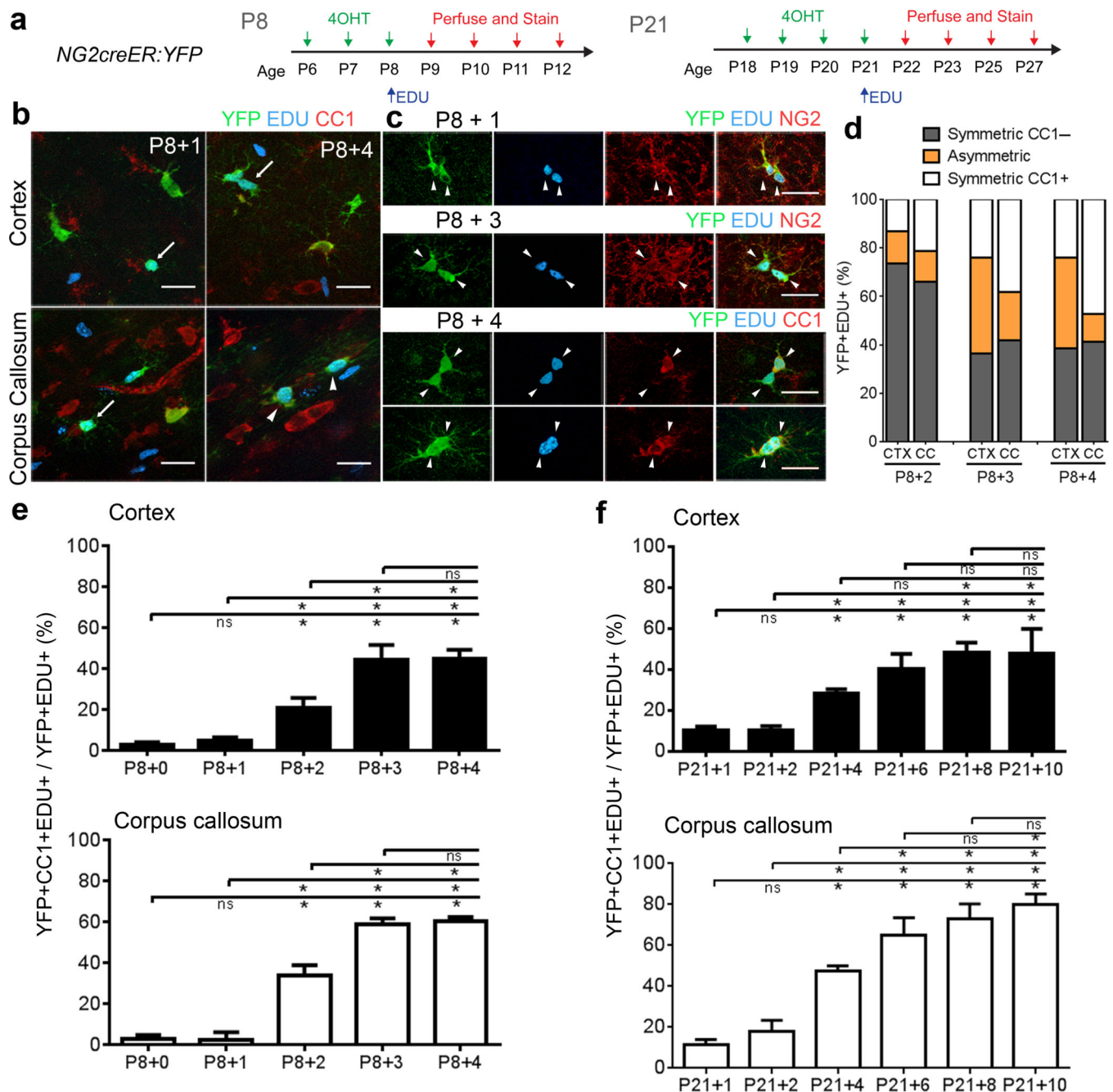
Figure 1. Temporal dynamics of oligodendrocyte differentiation after NG2 cell division *in vivo*
(**a**) Experimental protocol for EDU pulse-chase labeling in P8 and P21 *NG2creER:YFP* mice. (**b**) Labeling for YFP, EDU, and CC1 at 1 and 4 days after EDU injection. Arrows: YFP+EDU+CC1- cells, Arrowheads: YFP+EDU+CC1+ cells. (**c**) YFP+EDU+ cortical cell pairs immunostained for NG2 or CC1. Scale Bars in b–e 25μm. (**d**) The proportion of symmetric CC1– (two CC1–cells), symmetric CC1+ (two CC1+ cells), or asymmetric (one CC1+ and one CC1–cell) divisions in the cortex (CTX) and corpus callosum (CC) 2, 3 and 4 days after EDU injection. (**e**) Percentage of YFP+EDU+ cells that were CC1+ at the indicated days after EDU injection at P8. Cortex 0→2 *p=0.0002, t=5.554, 0→3 *p<0.0001,

t=12.92, 0→4 *p<0.0001, t=13.04, 1→2 *p=0.0008, t=4.946, 1→3 *p<0.0001, t=12.32, 1→4 *p<0.0001, t=12.43, 2→3 *p<0.0001, t=7.370, 2→4 *p<0.0001, t=7.483; Corpus Callosum 0→2 *p<0.0001, t=9.639, 0→3 *p<0.0001, t=17.34, 0→4 *p<0.0001, t=17.73, 1→2 *p<0.0001, t=9.800, 1→3 *p<0.0001, t=17.50, 1→4 *p<0.0001, t=17.89, 2→3 *p<0.0001, t=7.701, 2→4 *p<0.0001, t=8.094. **(f)** Percentage of YFP+EDU+ cells that were CC1+ after EDU injection at P21. Cortex 1→4 *p=0.0269, t=3.427, 1→6 *p<0.0001, t=6.616, 1→8 *p<0.0001, t=7.277, 1→10 *p<0.0001, t=7.160, 2→4 *p=0.0281, t=3.410, 2→6 *p<0.0001, t=6.597, 2→8 *p<0.0001, t=7.261, 2→10 *p<0.0001, t=7.143, 4→8 *p=0.0086, t=3.850, 4→10*p=0.0119, t=3.733; Corpus Callosum 1→4 *p<0.0001, t=6.868, 1→6 *p<0.0001, t=11.77, 1→8 *p<0.0001, t=11.73, 1→10 *p<0.0001, t=13.09, 2→4 *p<0.0001, t=5.619, 2→6 *p<0.0001, t=10.33, 2→8 *p<0.0001, t=10.48, 2→10 *p<0.0001, t=11.84, 4→6 *p=0.0088, t=3.843, 4→8 *p=0.0005, t=4.862, 4→10 *p<0.0001, t=6.226, 6→10 *p=0.0333, t=3.346. n=3 mice per group and genotype. Error Bars = SD. (*two-way ANOVA, Bonferroni post test).
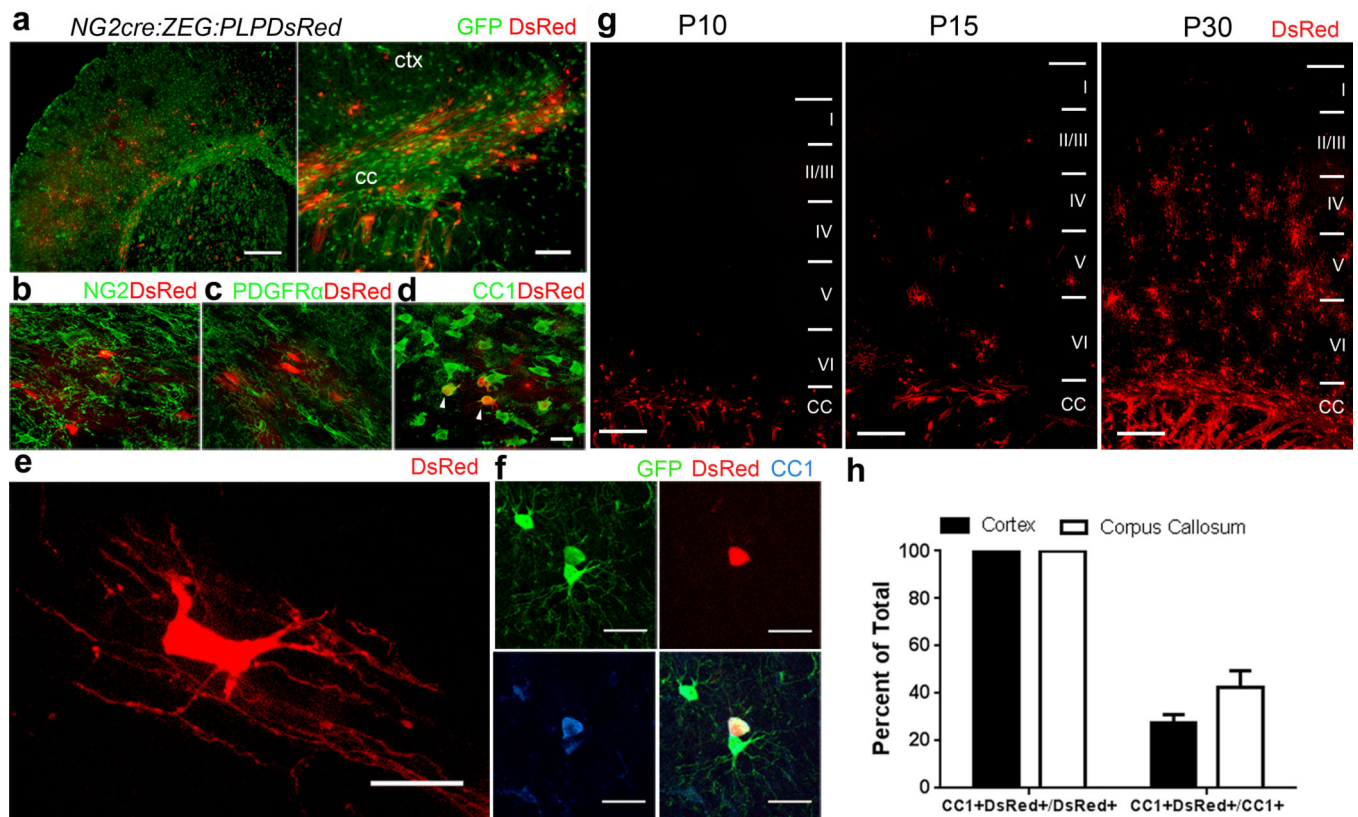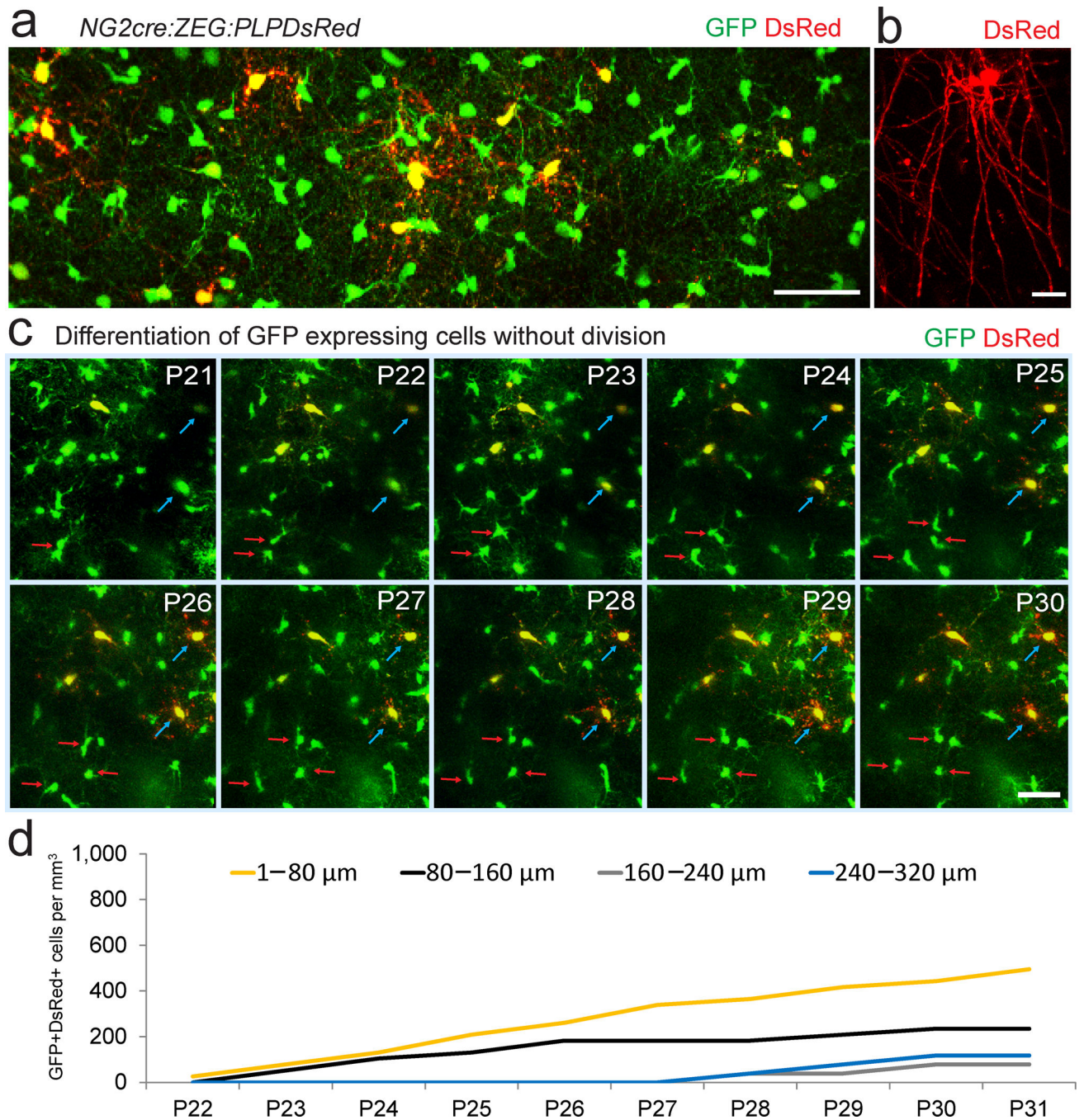
Figure 2. *NG2cre:ZEG:PLPDsRed* **triple transgenic mice identify cells at distinct stages of oligodendrocyte differentiation**

(a) Low magnification images taken from the forebrain of fixed tissue from P15 *NG2cre:ZEG:PLPDsRed* transgenic mice. **(b–d)** High magnification images taken from P15 corpus callosum immunostained for NG2 (b), PDGFRα (c) or CC1 (d) showing DsRed fluorescence in a subpopulation of CC1+ cells (arrowheads) but not in NG2 cells that are NG2+ or PDGFRα+. **(e)** High magnification image of a DsRed+ oligodendrocyte in the corpus callosum showing typical myelinating oligodendrocyte morphology with multiple parallel processes. **(f)** Example of a cortical GFP+DsRed+ cell that is also CC1+. **(g)** Low magnification images of DsRed expression at P10, P15 and P30 in the cortex (layers I–VI) and corpus callosum (CC) showing the increase in the density of DsRed expressing oligodendrocytes during the first month of postnatal development. Scale bars 100 μm and 50 μm in a, 25μm in b–d and 250μm in g. **(h)** Quantification in *PLPDsRed* transgenic mice demonstrating that DsRed+ cells represent a minor subset of CC1+ cells in the cerebral cortex and corpus callosum. Error bars = SD.
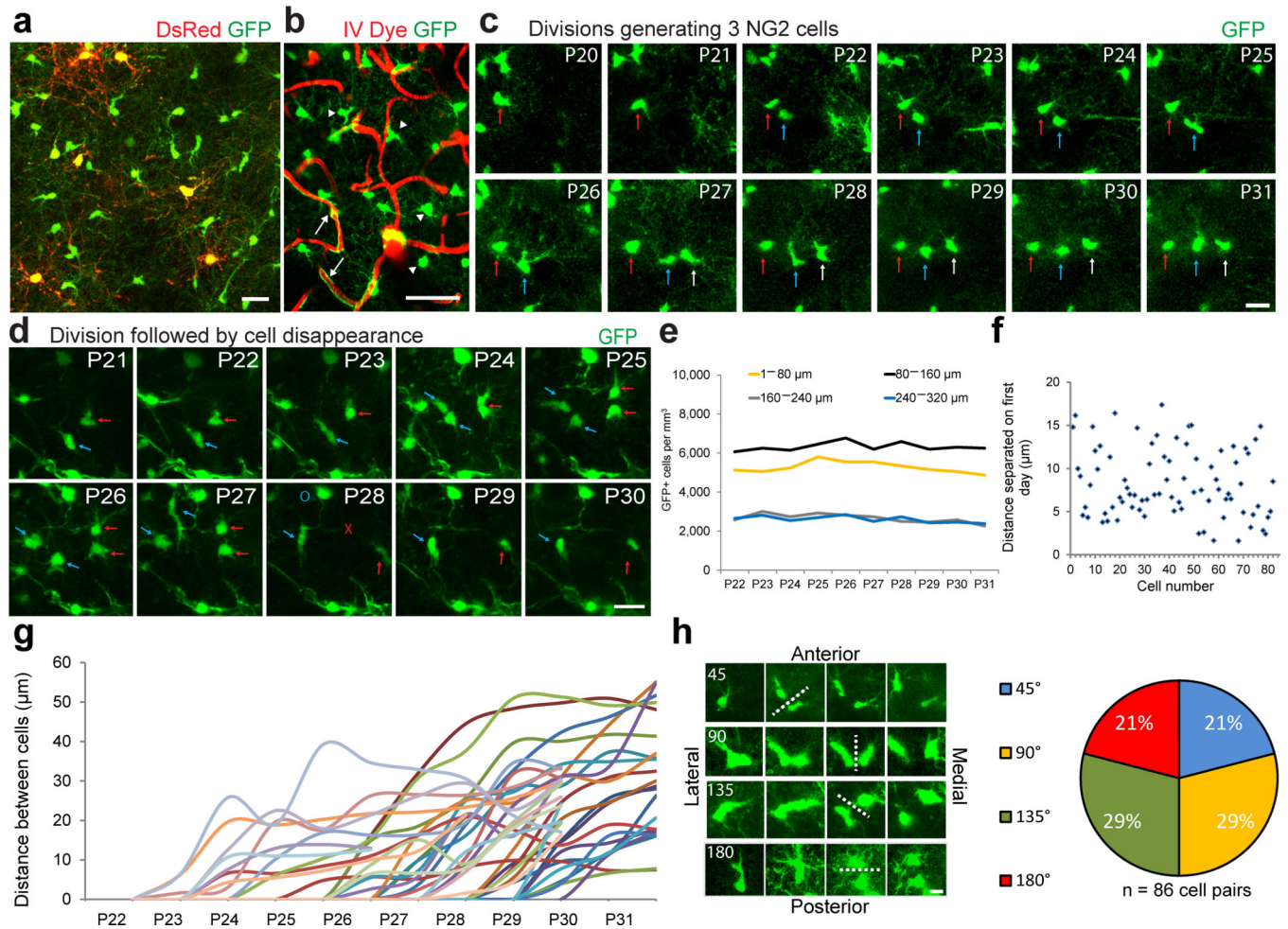
Figure 3. Longitudinal *in vivo* imaging of cortical NG2 cells

(**a**) Example *in vivo* two-photon image captured with 975nm laser excitation from a P25 *NG2cre:ZEG:PLPDsRed* triple transgenic mouse. (**b**) Image captured *in vivo* from the somatosensory cortex of an *NG2cre:ZEG* transgenic mouse intravenously injected with Texas Red dextran to visualize the cortical vasculature showing the distinction and identification of GFP+ (green) NG2 cells (arrowheads) and vascular pericytes (arrows). Scale Bar = 50μm. (**c**) Montage of images of the same GFP+ NG2 cells captured daily from P20–P31, showing two cell divisions (arrows) over the imaging period. Scale Bar = 20μm. (**d**) Montage of images captured from P21–P30 showing individual GFP+ cells dividing (arrows) and then disappearing (red X) or migrating out of the field of view (blue O) 4 days after division Scale Bar = 20μm. (**e**) The density of GFP+ cells from P22–P31 by cortical depth. (**f**) Graph showing the distance between individually divided GFP+ cell pairs one day after cell division. (**g**) Cell separation trajectories of a subset of imaged GFP+ cell divisions depicting the distance between divided cells over the imaging period. (**h**) Example images of four types of division angles relative to brain orientation, with dotted line indicating division plane and time of division. Scale Bar = 10 μm. Quantification of each type of division from 86 cell division events.

Figure 4. *In vivo* **imaging of oligodendrocyte differentiation**
(**a**) Two-photon fluorescence image captured *in vivo* from the somatosensory cortex from a
P35 *NG2cre:ZEG:PLPDsRed* transgenic mouse showing GFP+ NG2 cells, GFP+
oligodendrocytes, and GFP+ DsRed+ mature oligodendrocytes. Scale Bar = 50μm. (**b**) High
magnification *in vivo* image of a single DsRed+ oligodendrocyte showing the distinctive
morphology of a mature oligodendrocyte. Scale bar = 20μm. (**c**) Time-lapse sequence from
P21–P30 showing dividing GFP+ cells (red arrows) and other GFP+ cells gradually

becoming DsRed+ (blue arrows), but no GFP+ cell dividing and becoming DsRed+. Scale Bars = 50μm. **(d)** The density of GFP+DsRed+ cells appearing from P22–P31.
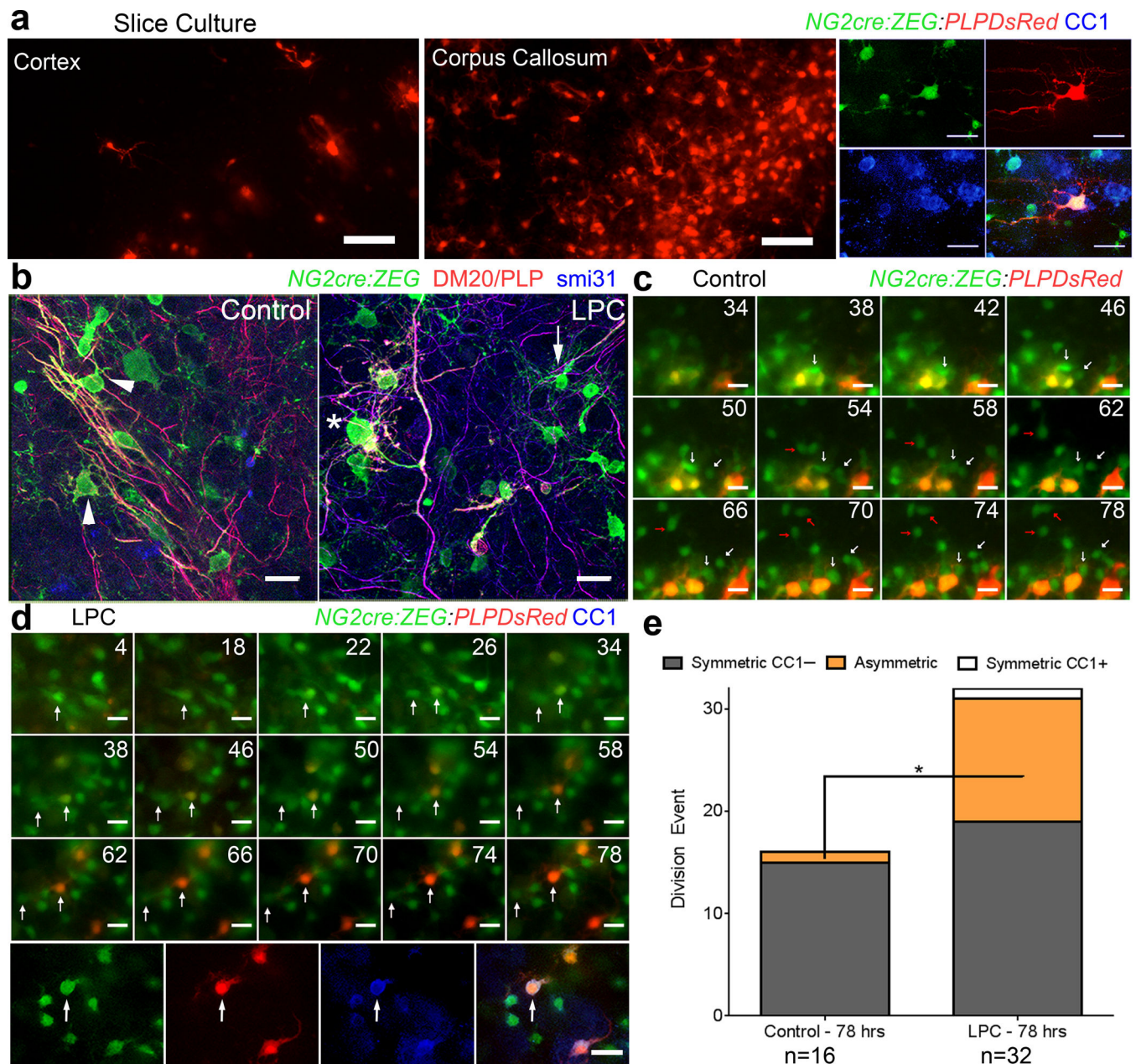
Figure 5. The temporal dynamics of oligodendrocyte differentiation are altered by myelin damage

(a) Images taken from control *NGcreZEG:PLPDsRed* slice cultures at the end of time-lapse imaging, showing DsRed expression in the cortex and corpus callosum, and an **e**xample of a GFP+DsRed+ gray matter oligodendrocyte expressing CC1 after post hoc immunostaining. Scale Bars = 50 μm top 25 μm bottom **(b)** Control and LPC -treated *NG2cre:ZEG* slices fixed at the beginning of time lapse imaging (31 hours after demyelination) and immunostained for DM20 (red) and phosphorylated neurofilaments (blue) showing relatively normal appearing GFP+DM20/PLP– cells (arrow) and GFP+DM20/PLP+ oligodendrocytes in LPC-exposed slices with degenerated processes (asterisk) compared with robust parallel processes extending along axons seen in control conditions

(arrowheads), images from corpus callosum. Scale Bars = 20 μm. **(c)** Montage of images from a control slice showing GFP+ (green) gray matter cells (arrows) dividing but not becoming DsRed+ (red) over the 78-hour imaging period (hours indicated in top right corner of each panel). Scale Bar = 20 μm. **(d)** Images captured over 78 hours after LPC treatment of cortical slice show a GFP+ gray matter NG2 cell (arrow) dividing and then differentiating and becoming DsRed+ 20 hours after division. Immunostaining after imaging demonstrated that the imaged GFP+DsRed+ cell was a CC1+ oligodendrocyte. Scale Bar = 20 μm. **(e)** Quantification from time-lapse imaging of control and LPC-treated slice culture showing a shift to asymmetric fate of divided GFP+ cells after LPC exposure. (*p = 0.0168, t = 2.815) unpaired Student's *t*-test.
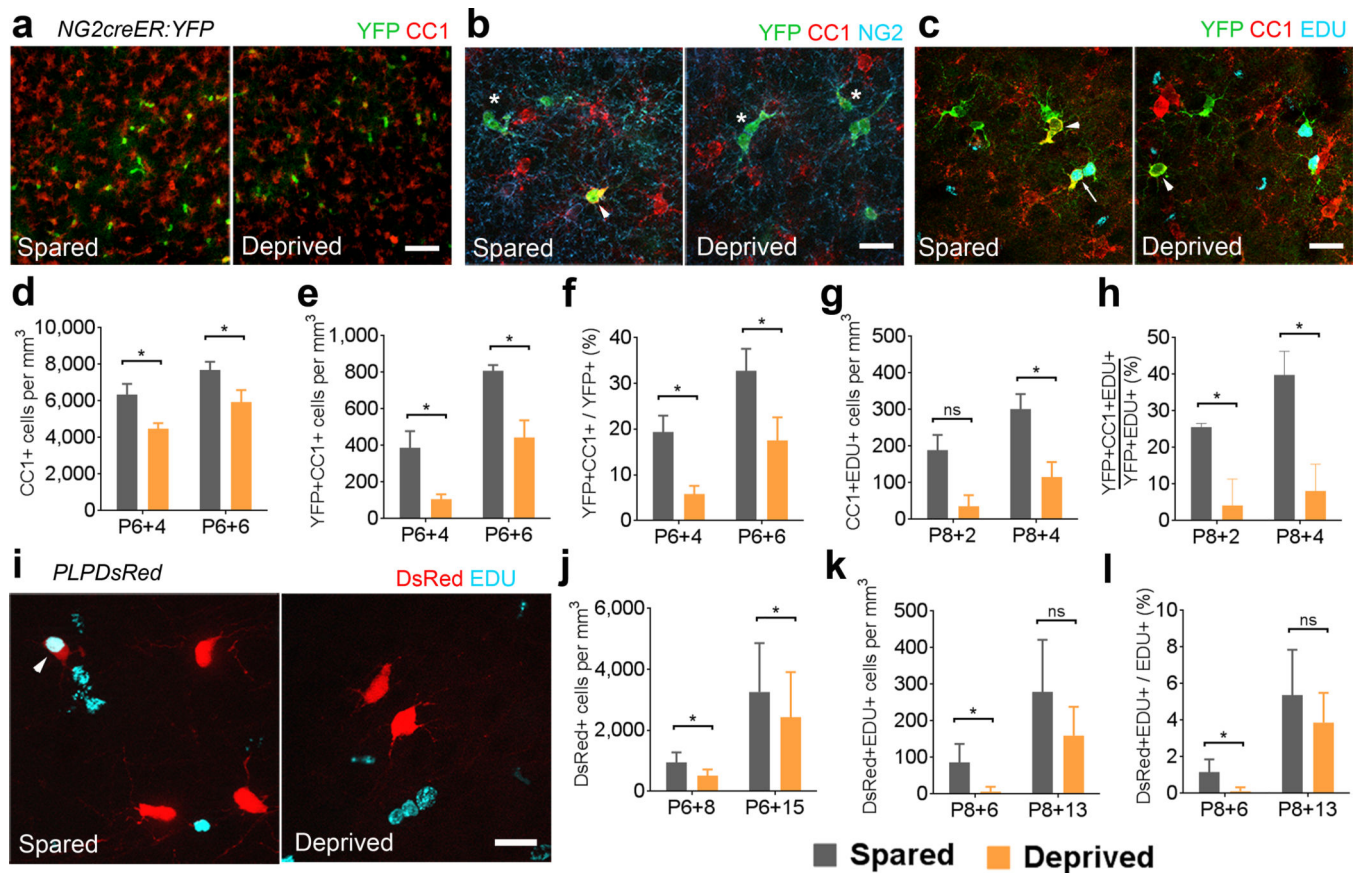
Figure 6. Whisker deprivation reduces oligodendrocyte generation in the somatosensory cortex
(**a**) Coronal sections through layer IV of spared and deprived somatosensory cortex immunostained for YFP and CC1. Scale bar = 50μm. (**b**) Layer IV immunostained for YFP, CC1 and NG2. Arrowhead: YFP+CC1+ cells. Asterisks: YFP+NG2+ cells. Scale bar = 25μm. (**c**) Layer IV labeled for YFP, CC1, and EDU. Arrow: YFP+CC1+EDU+ cell. Arrowheads: YFP+CC1+ cells. Scale bar = 25μm. (**d**) Comparison of the density of CC1+ cells between spared and deprived layer IV at P6+4 (*p=0.0079, t=11.18) and P6+6 (*p=0.0108, t=9.526). (**e**) The density of YFP+CC1+ cells in layer IV at P6+4 (*p=0.0213, t=6.748) and P6+6 (*p=0.0247, t=6.243). (**f**) The proportion of YFP+ cells that were CC1+ at P6+4 (*p=0.0227, t=6.474) and P6+6 (*p=0.0132, t=8.604). (**g**) The density of CC1+EDU+ cells at P8+2 (p=0.0505, t=4.281) and P8+4 (*p=0.0447, t=4.570) (**h**) The proportion of YFP+EDU+ cells that were CC1+ at P8+2 (*p=0.0273, t=5.944) and P8+4 (*p=0.0009, t=33.18). (**i**) Images of spared and deprived somatosensory cortex of *PLPDsRed* mice showing EDU labeling and DsRed fluorescence. Scale bar = 25μm (**j**) Density of DsRed+ cells in *PLPDsRed* mice at P6+8 (*p=0.0074, t=6.523) and P6+15 (*p=0.0120, t=5.469). (**k**) The density of DsRed+EDU+ cells at P8+6 (*p=0.0248, t=4.324) and P8+13 (p=0.0582, t=2.987). (**l**) The proportion of EDU+ cells that were also DsRed+ at P8+6 (*p=0.0231, t=4.301) and P8+13 (p=0.0937, t=2.426). *paired Student's *t*-test. Error bars = SD. n=3 or 4 mice per age group.
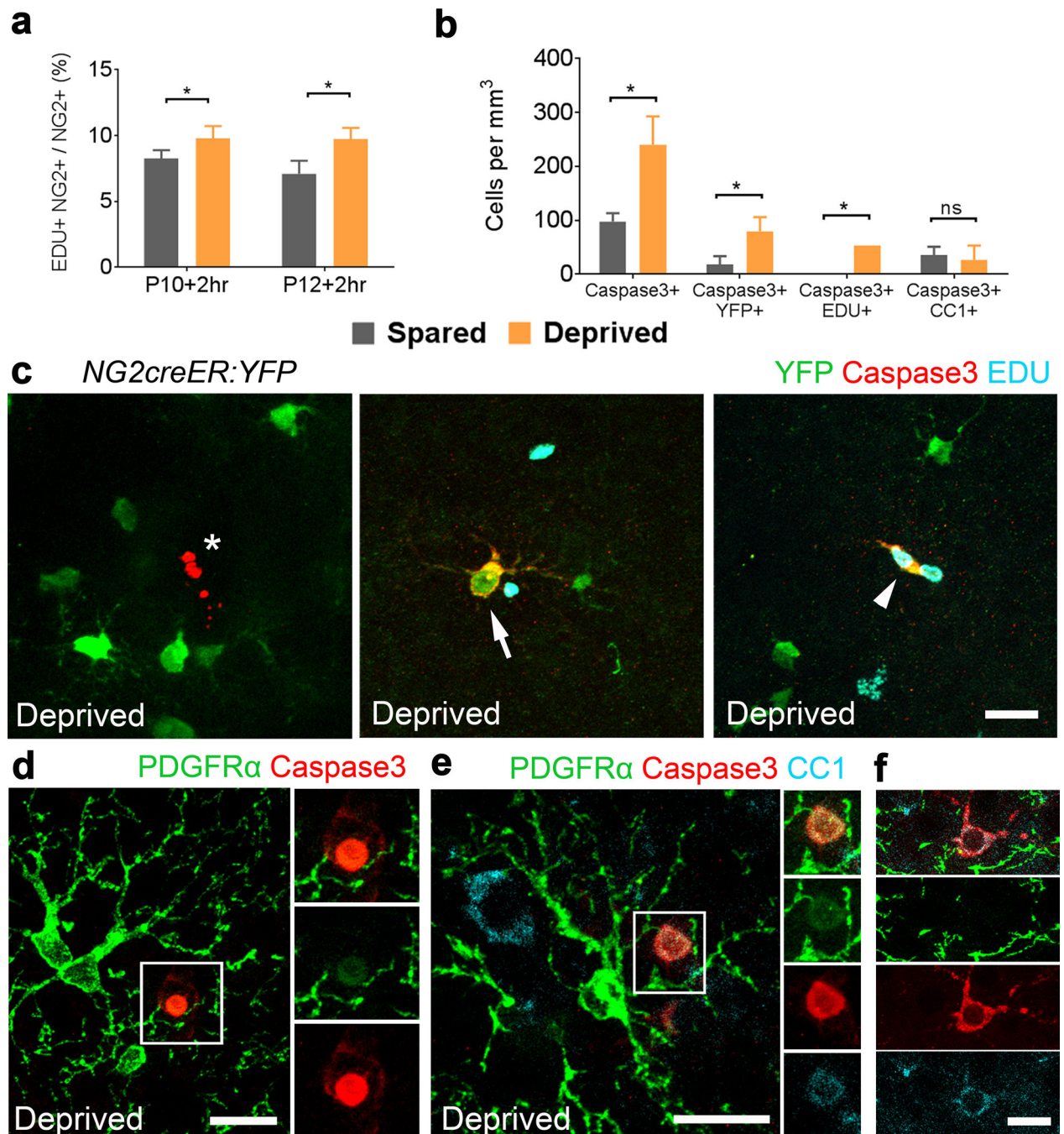
Figure 7. Whisker sensory deprivation increases apoptosis of divided NG2 cells
(a) The proportion of EDU+ NG2+ cells in spared and deprived somatosensory cortices after whisker clipping at P10 (*p=0.0379, t=4.986) and P12 (*p=0.0451, t=4.548). **(b)** Comparison of the density of Caspase-3+ (*p=0.0255, t=6.140), Caspase-3+YFP+ (*p=0.0192, t=7.115), Caspase-3+EDU+ (*p=0.0000) and Caspase-3+CC1+ (p=0.7359, t=0.3872) cells in spared and deprived cortices of NG2creER:YFP mice. **(c)** Example images from the deprived somatosensory cortex showing an unlabeled Caspase-3+ cell with typical apoptotic morphology (left, asterisk), a Caspase-3+ YFP+ cell (middle, arrow), and a

Caspase-3+ EDU+ YFP+ cell (right, arrowhead). Scale bar = 20 μm. **(d–f)** Example images from deprived somatosensory cortex immunostained for PDGFRα, Caspase-3 and CC1. Scale bars = 20μm. *paired Student's *t*-test. Error bars = SD. n=3 mice per age group.